Modeling the Formation of Boron Carbide Particles in an Aerosol Flow Reactor

Yun Xiong and Sotiris E. Pratsinis
Dept. of Chemical Engineering, Center for Aerosol Processes, University of Cincinnati, Cincinnati, OH 45221

Alan W. Weimer
Ceramics and Advanced Materials Research, Dow Chemical U.S.A., Midland, MI 48674

The formation of submicron crystals of boron carbide (B_4C) by coagulation and sintering by the rapid carbothermal reduction of intimately mixed carbon-boron oxide powders in an aerosol flow reactor at temperatures above the boiling point of boron oxide is investigated. High heating rates (10^5 K/s) force rapid evaporation of boron oxide and suboxides from the precursor powder, resulting in its rupture and formation of boron carbide molecular clusters that grow to macroscopic particles by coagulation. Consequently, the formation and growth of B_4C particles are described by simultaneous interparticle collision and coalescence using a two-dimensional particle-size distribution model that traces the evolution of both size and shape characteristics of the particles through their volume and surface area. In addition to the coagulation term, the governing population balance equation includes a coalescence contribution based on B_4C sintering law. The predicted evolution of the two-dimensional particle-size distribution leads to a direct characterization of morphology as well as the average size and polydispersity of the powders. Furthermore, model predictions of the volume and surface area of boron carbide particles can be directly compared with experimental data of B_4C specific surface area and an effective sintering rate of B_4C is deduced.

Introduction

Boron carbide is known for its hardness and chemical resistance. It has a high cross section for neutron absorption due to its high boron content. Because of its high hardness, it is useful in applications such as armor plating and the production of mechanical mold, diemaker polishing stones, and cutting and grinding tools. It is also used in the shielding and control of nuclear reactors because of its neutron absorptivity, chemical inertness, and radiation stability. Therefore, there is substantial interest in the manufacture of boron carbide, particularly powders composed of fine, submicron crystallites. Boron carbide fabricated parts consisting of fine grains are significantly stronger than parts consisting of coarse grains (Osipov, 1982). Conventional methods for manufacturing boron carbide involve the reduction of boron oxide with carbon either in a batch electric arc furnace (Lipp, 1965) or with magnesium metal by the thermite reaction (Gray, 1958). These processes are characterized by slow, nonuniform heating, chemical impurities, and subsequent processing complications. One effective method to avoid the above problems is direct synthesis of submicron-size powders from laser-heated or plasma-heated gaseous precursors (Cannon et al., 1982; Mackinnon and Reuben, 1975). The nearly instantaneous rates of both reactant heating and product cooling as well as the short and uniform reaction times result in submicron, uniformly sized B_4C particles. However, the high cost of the processing equipment and gaseous raw materials (for example, BCl_3) does not favor industrial scale manufacture of gas phase synthesized B_4C powders.

Recently, Weimer et al. (1991) described a rapid carbothermal reduction process in a flow reactor configuration for continuously manufacturing submicron crystals of boron carbide. This process approaches the uniformity and rapid tem-

Correspondence concerning this article should be addressed to S. E. Pratsinis.

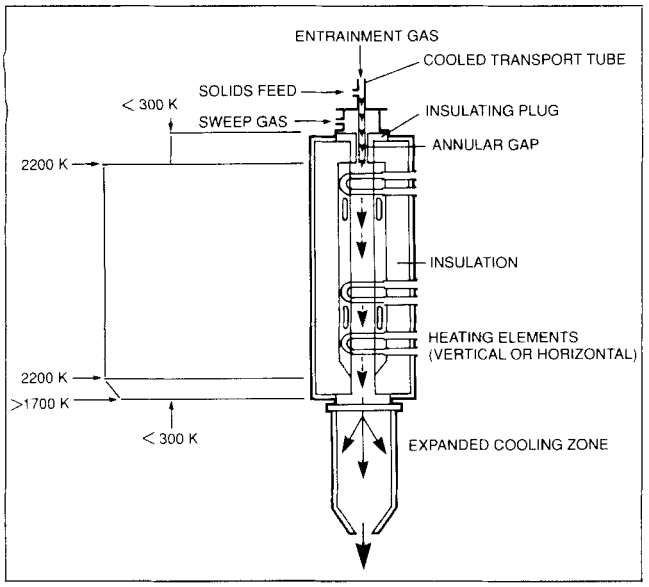

Figure 1. Aerosol flow reactor for boron carbide manufacture by rapid carbothermal reduction (Weimer et al., 1991).

perature differentials of the gas phase laser- and plasma-heated routes, but at a substantially lower cost. In this process, a uniform solid mixture of calcined corn starch (carbon "soot") and boron oxide made from liquid precursors is milled to particles of less than 45 μm. These particles are suspended in argon gas and fed into a 0.14 m ID $\times$ 1.68 m long graphite flow reactor which is maintained at approximately 2,200 K (Figure 1). Additional argon gas is fed around the particle inlet

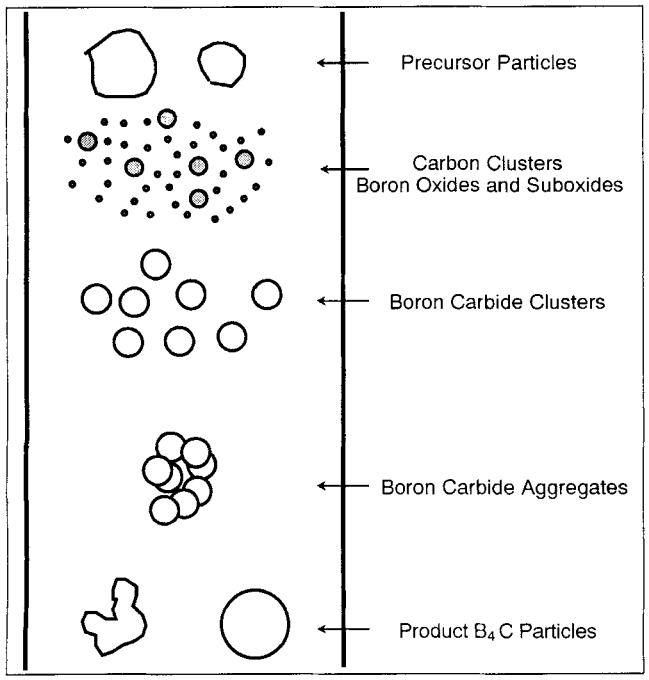

Figure 2. Formation and growth of B_4C particles along the reactor.

to mitigate deposits to reactor walls. The precursor particles contain carbon and boron oxide in stoichiometric amounts that convert to boron carbide according to:

$$7C(s) + 2B_2O_3(l, g) = B_4C(s) + 6CO(g) \quad (1)$$

As the particles enter the reactor they are heated to a temperature which is below the boiling point of carbon but above the boiling point of boron oxide, 2,133 K (Weast et al., 1986). The reactor temperature is also above the temperature, 1,733 K, at which liquid boron oxide is reduced to gaseous boron oxide in the presence of carbon (Lamoreaux et al., 1987):

$$C(s) + B_2O_3(l) = B_2O_2(g) + CO(g) \quad (2)$$

$$5C(s) + 2B_2O_2(g) = B_4C(s) + 4CO(g) \quad (3)$$

As a result, rapid heating (10^5 K/s, Weimer et al., 1992) promotes rapid volatilization of B_2O_3 and release of CO from the precursor particles, forcing particle rupture in a similar fashion to the breakup of coal particles in pulverized coal combustion (Celik et al., 1990). The uniform particle composition may support a thorough particle breakup and rapid reaction between boron and carbon leading to formation of B_4C clusters by reaction 3 and/or 1 that grow to macroscopic particles by coagulation as schematically shown in Figure 2. Rapid cooling in an expanded cooling zone at the end of the reactor ceases particle coalescence. As a result, no particle growth takes place outside the reactor.

Assuming instantaneous breakup of precursor particles and formation of boron carbide clusters, particle formation and growth can be modeled by simultaneous coagulation and coalescence (Figure 2). This assumption applies best at process temperatures above 2,133 K (Weimer et al., 1992). The relative rate of interparticle collision and coalescence (sintering) determines particle morphology. Early in the process, sintering of small particles is much faster than collision resulting in spherical particles. As particles grow further, the characteristic time for sintering increases substantially so particle coalescence can no longer be regarded as instantaneous with respect to particle collision. Consequently irregularly shaped B_4C particles (agglomerates) are formed. Theoretical studies of aerosol dynamics are largely confined to spherical particles, though in some studies shape factors have been used to correct the deviation of particle properties from those of ideal spheres. Recently, Xiong and Pratsinis (1991b) developed a two-dimensional particle-size distribution model that can trace the evolution of both the volume and surface area of aerosol particles during gas-phase powder production accounting for particle coagulation and sintering. Using volume and surface area as the two particle dimensions, the aerosol dynamic equations are solved by extending a one-dimensional sectional technique (Xiong and Pratsinis, 1991a) to the two-dimensional particle-size space. The simultaneous prediction of the evolution of the particle volume and surface area distribution leads to a direct characterization of the agglomerates (or aggregate particles) and the grains (or crystallites or primary particles).

This article studies formation and growth of boron carbide particles by coagulation and sintering in the rapid carbothermal reduction process using the above two-dimensional particle-

size distribution model. The predicted B_4C grain (crystallite) sizes are compared with experimental data.

Theory

A two-dimensional particle-size distribution function is defined as $n_t(v, a)$ where $n_t(v, a)dadv$ is the number density of particles having volume between v and $v+dv$ and surface area in the range a to $a+da$ at time t. For an aerosol that is rapidly formed by gas phase reaction at high temperatures, the rate of change in $n_t(v, a)$ is given by the rate of simultaneous coagulation and coalescence among aerosol particles. The two-dimensional population balance equation can be written in a continuous form as (Koch and Friedlander, 1990; Xiong and Pratsinis, 1991b, 1993):

$$\frac{\partial n_t(v, a)}{\partial t}=\frac{1}{2}\int_0^v \theta\left(a>\left(\frac{\bar{v}}{v_0}\right)^{2/3}a_0+\left(\frac{v-\bar{v}}{v_0}\right)^{2/3}a_0\right)$$

$$\times\int_{\left(\frac{\bar{v}}{v_0}\right)^{2/3}a_0}^{\frac{\bar{v}}{v_0}a_0}\beta_{\bar{v},v-\bar{v}}(\bar{a}, a-\bar{a})n_t(\bar{v}, \bar{a})n_t(v-\bar{v}, a-\bar{a})d\bar{a}d\bar{v}$$

$$-n_t(v, a)\int_0^\infty\int_{\left(\frac{\bar{v}}{v_0}\right)^{2/3}a_0}^{\frac{\bar{v}}{v_0}a_0}\beta_{v,\bar{v}}(a, \bar{a})n_t(\bar{v}, \bar{a})d\bar{a}d\bar{v}$$

$$+\frac{1}{\tau_f}\frac{\partial}{\partial a}\left(\left[a-\left(\frac{v}{v_0}\right)^{2/3}a_0\right]n_t(v, a)\right) \quad (4)$$

where v_o and a_o are the volume and surface area respectively, of a primary spherical particle. An agglomerate of volume v is thus composed of v/v_o primary particles. Its surface area lies between that of a perfect sphere when complete coalescence has taken place, $(v/v_o)^{2/3}a_o$, and that of an aggregate of primary particles just touching one another, $(v/v_o)a_o$.

The first righthand-side (RHS) term of Eq. 4 accounts for the gain of particles of volume v and surface area a by coagulation of smaller particles. The step function θ is introduced because a particle of volume v produced by collision between particles of volume $\bar{v}$ and $v-\bar{v}$ cannot have upon contact surface area less than the sum of the surface area of the two particles. Only coalescence can reduce the resulting particle surface area to the theoretical minimum—that of a sphere of volume v. The second RHS term in Eq. 4 accounts for the loss of particles of volume v and surface area a by coagulation with all other particles. The collision frequency function β depends on both particle size and shape which are quantitatively represented by the particle volume and surface area in the present model. For each agglomerate, a spherical equivalent is identified that has a surface area equal to the accessible surface area of the irregularly shaped particle. Thus, the diameter of this equivalent sphere, d_a, is given by:

$$d_a=\sqrt{sa/\pi} \quad (5)$$

where s is the surface area accessibility which again is a function of the particle size and shape. A measure of the particle size can be obtained from the particle volume and a quantitative estimate of the particle shape can be deduced from the surface fractal dimension, D_s (Mandelbrot, 1983):

$$\frac{a}{a_0}\sim\left(\frac{v}{v_0}\right)^{D_s/3} \quad (6)$$

The D_s ranges from 2 to 3: $D_s=2$ for completely fused spheres and $D_s=3$ in the absence of sintering, an ultimately porous particle. To obtain a quantitative expression for s note that $s=1$ when $D_s=2$ (dense spheres). For $D_s=3$, s can be related to the cluster size ($i=v/v_o$) through a surface area scaling factor α which is defined as (Meakin and Witten, 1983):

$$j\sim i^\alpha \quad (7)$$

where j is the number of surface grains that are exposed to diffusing particles surrounding the cluster. Hence, the surface area accessibility of cluster i is:

$$s=\frac{a_0 j}{a_0 i}=\frac{j}{i} \quad (8)$$

Combining Eqs. 7 and 8, one obtains for $D_s=3$:

$$s\sim\frac{1}{i^{1-\alpha}} \quad (9)$$

The value of α depends on both material and growth kinetics of the cluster. From computer simulation of diffusion limited aggregation (DLA), Meakin and Witten (1983) obtained $\alpha=0.74$ indicating that a relatively close-packed structure is formed by the diffusion of spherical particles to the cluster and an appreciable portion of the surface area is shielded (unexposed). However, particle coagulation in practical systems involves cluster-cluster (CC) as well as monomer-cluster (MC) aggregation (Schaefer and Hurd, 1990) and CC growth is known to produce more open structures (Meakin, 1984). Indeed, Schmidt-Ott (1988) obtained a value of 0.92 from *in situ* characterization of ultrafine silver agglomerates formed by coagulation.

Since s is unity for $i=2$, one can normalize Eq. 9 to obtain:

$$s=\left(\frac{2}{i}\right)^{1-\alpha} \quad \text{for } D_s=3 \quad (10)$$

For the entire range of D_s a linear interpolation between $D_s=2$, and $D_s=3$ through Eq. 10 relates s to i and D_s as:

$$s=(D_s-2)\left(\frac{2}{i}\right)^{1-\alpha}+3-D_s \quad (11)$$

In the present simulations, α is taken to be 0.8. The Fuchs expression for the Brownian coagulation coefficient covering the whole size regime (Fuchs, 1964; Table 10.1 in Seinfeld, 1986) is used to evaluate β of irregularly shaped particles based on their corresponding surface area equivalent sphere diameter.

The third righthand-side term in Eq. 4 is the sintering con-

tribution related to the material sintering mechanism through the continuity equation (Koch and Friedlander, 1990):

$$\left[\frac{\partial n_l(v, a)}{\partial t}\right]_{\text{sintering}} = \frac{-\partial}{\partial a}\left[\frac{da}{dt} n_l(v, a)\right] \tag{12}$$

The sintering rate is expressed by the surface area reduction rate:

$$\frac{da}{dt} = -\frac{1}{\tau_f}(a - a_{\text{final}}) \tag{13}$$

where a_{final} is the surface area of the completely fused sphere, that is, $(v/v_o)^{2/3}a_o$. The characteristic coalescence time, τ_f, depends on the B_4C sintering mechanism. The strong covalent bonding, low plasticity, high resistance to grain boundary sliding and low solid-state superficial tension of B_4C hinder the sintering of B_4C in synthesis of dense products (Thevenot, 1988). Consequently, pressureless sintering of pure B_4C often exhibits microscopic coarsening without densification as a result of greater transport of matter by surface diffusion than by volume and/or grain-boundary diffusion (Greskovich and Rosolowski, 1976). Microscopic coarsening can be avoided by using ultrafine powders which result in both shorter diffusion distances and higher effective stresses at pore/solid interfaces and by using sintering additives. In the present study the former is more applicable (Weimer et al., 1991).

Boron carbide and other covalently-bonded solids such as SiC and Si_3N_4 sinter by solid-state diffusional processes (Greskovich and Rosolowski, 1976). For solid-state diffusion, the characteristic sintering time of two equal-sized grains of diameter d_g is given by (Kingery et al., 1976):

$$\tau_f \alpha \frac{k_B T}{D^* \Omega \gamma} d_g^3 \tag{14}$$

where D^* is the self-diffusion coefficient for the mobile species, Ω is the atomic volume of the diffusing material, and γ is the surface energy. There is little data on pressureless sintering of boron carbide in the absence of additives and to the best of the authors' knowledge, the D^* and γ of B_4C have not been reported in the literature. So in the absence of firm and precise literature data, B_4C property data (D^* and γ) can be inferred and estimated from sintering experiments in the literature of other covalent solids. Extensive experimental studies indicate that addition of small amounts of B, C, Si, combinations or covalent compounds of these elements promotes pressureless sintering of B_4C and SiC (Thevenot, 1988; Hase and Suzuki, 1981; van Rijswijk and Shanefield, 1990; Lange and Gupta, 1976). Excess carbon actively enhances self-diffusion in both SiC and B_4C. van Rijswijk and Shanefield (1990) showed that in a carbon-rich atmosphere, the bulk-diffusion rate of silicon substantially increases such that carbon self-diffusion becomes slower and, as a result, rate controlling. This results in a 100-fold increase in the overall self-diffusion rate of SiC. If excess carbon has the same effect on boron carbide self-diffusion as it would in the early stages of B_4C carbothermal reduction where carbon is abundant, the silicon carbide self-diffusion coefficient in a carbon-rich atmosphere can be used as a first approximation in estimating the B_4C sintering rate. From Figure 1 of van Rijswijk and Shanefield (1990), an expression for the B_4C self-diffusion coefficient is deduced as:

$$D^* = 0.3\exp\left[-\frac{53{,}648}{T}\right] \tag{15}$$

The carbon vacancy volume is calculated as 3.64×10^{-23} cm^3.

The surface energy of B_4C also needs to be estimated from related compounds, preferably covalant carbides such as SiC and TiC. Livey and Murray (1956) found that the surface energies of the carbides of Zr, U, Ti and Ta show a linear relationship with the heat of formation of these carbides. They reported the surface energy of TiC at 1,373 K as $1{,}190 \pm 350$ dyne/cm. Assuming that B_4C and SiC also follow approximately the same relationship, then their surface energies can be estimated from their heat of formation and the surface energy and heat of formation of the refractory monocarbides. Dean (1985) gives the heat of formation values for B_4C, SiC and TiC as -17, -17.5, -44.0 kcal/mol, respectively. According to the above reasoning, B_4C and SiC should have about the same surface energy: $\sim 1{,}000$ dyne/cm. Using these estimated values of D^* and γ, a quantitative expression of the characteristic coalescence time for B_4C is obtained:

$$\tau_f = 39 T d_g^3 \exp\left[\frac{53{,}648}{T}\right] \tag{16}$$

where a constant 1/40 is used to equate Eq. 14 (Kingery et al., 1976: page 476).

In the present study, two equivalent particle diameters, d_p and d_g, are used to quantitatively describe the agglomerate size and morphology, respectively. The agglomerate size or the equivalent solid sphere diameter of an agglomerate, d_p, is defined as the diameter of a coalesced sphere having the same particle volume as the agglomerate:

$$d_p = \left(\frac{6v}{\pi}\right)^{1/3} \tag{17}$$

The average grain diameter of the agglomerate, d_g, can be obtained from its volume and surface area:

$$d_g = \frac{6v}{a} \tag{18}$$

Equation 4 is a two-dimensional partial integro-differential equation that needs to be solved numerically. A one-dimensional sectional method (Gelbard et al., 1980; Xiong and Pratsinis, 1991a) is extended to include the surface area dimension (Xiong and Pratsinis, 1991b). This results in a set of ordinary differential equations (ODEs) that are solved using an efficient ODEs solver, subroutine IVPAG (IMSL, 1989). A complete listing of the computer program is given by Xiong (1992).

Results and Discussion

Table 1 (Weimer et al., 1991) lists the experimental runs made at reactor temperatures above the boiling point of boron oxide ($\sim 2{,}133$ K). Precursor powders were fed to the cooled

Table 1. Characteristics of Boron Carbide Powders and Experimental Conditions (Weimer et al., 1991)

Run No.	Argon Flow, F_g g/s	T K	t (Exp.) s	t (Calcul.) s	Specific Surface Area, A m^2/g	Avg. Grain Size, d_g μm
38-24	3.03	2,173	1.3	1.1	24.4	0.098
97-42	6.74	2,223	0.7	0.64	17.7	0.13
58-31	6.06	2,273	0.7	0.68	12.5	0.19
35	5.32	2,373	0.75	0.71	N/A	~0.2

$F_s = 2$ g/s

flow tube at the rate $F_s = 2$ g/s and swept into the reaction chamber with argon gas (Figure 1) flowing at rate F_g. At the employed reactor temperatures, complete carbon conversion to stoichiometric B_4C was achieved. In model simulations, the velocity distribution in the reactor is approximated as one-dimensional plug flow to simplify the calculations. The gas phase is a mixture of inert gas Ar and reaction product CO at an approximately 2 to 1 molar ratio as dictated by the powder feed, overall chemical reaction (Eq. 1) and argon flow rates. Hence, residence times based on the ideal gas law can be calculated (Table 1: Column 5) and used in the simulations and the calculation of transport properties such as gas density and viscosity (Reid et al., 1987) in the reactor. From the measured specific surface area at various reactor temperatures (Table 1), the experimentally determined average B_4C grain sizes can be obtained:

$$d_g = \frac{6}{\rho_p A} \tag{19}$$

where the particle density ρ_p is 2.52 g/cm^3 for B_4C and A is the measured specific surface area. For the powder collected at 2,373 K (Run 35), specific surface area data were not available so d_g is estimated from micrographs of product B_4C powders (for example, Figure 5). All simulations are carried out under isothermal conditions at 1 atm. The smallest possible primary particle is that of a B_4C molecule, so v_o is 3.64×10^{-23} cm^3.

Since the powder feeding rate was kept constant in the experiments, the average size and morphology of product B_4C powders are only affected by the argon flow rate and reactor temperature. A higher argon flow rate means a shorter reactor residence time, resulting in smaller average agglomerate particle sizes. While increasing temperature enhances the coagulation rate ($\beta\alpha T^{1/2}$), it decreases the residence time more profoundly ($t\alpha T^{-1}$). Consequently, for a given argon flow rate the agglomerate particle size decreases with increasing temperature. With respect to particle morphology, increasing both the reactor residence time and temperature promotes coalescence and subsequently increases the grain/crystallite size of the final product.

Figure 3 shows two snapshots of the number density of B_4C agglomerates in the two-dimensional space of particle volume and surface area at 2,173 K (Run 38-24) and residence times 0.3 s and 1.1 s, respectively. The total number of agglomerate B_4C particles is reduced by coagulation and consequently the average agglomerate size increases as the residence time increases from 0.3 to 1.1 s. It is worth noting that coagulation greatly depletes the small particles but does very little in increasing the number of the large ones over this time period. The two-dimensional distribution is bound by two solid lines in Figure 3. The diagonal line on the (v, a) plane corresponds to agglomerates consisting of primary particles just touching one another upon collision without sintering. This line can be termed the collision line. The other solid line in the (v, a) plane

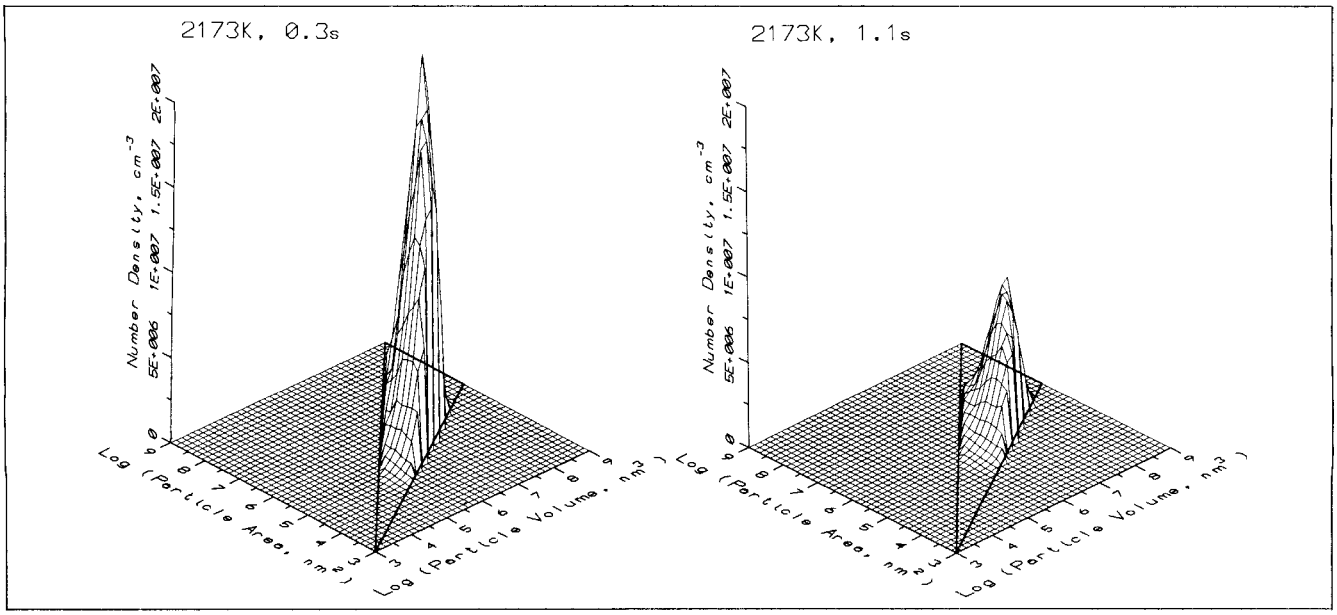

Figure 3. Number density of B_4C agglomerates at 2,173 K (Run 38-24) and residence times 0.3 s and 1.1 s, respectively, in the two-dimensional space of particle volume and surface area.

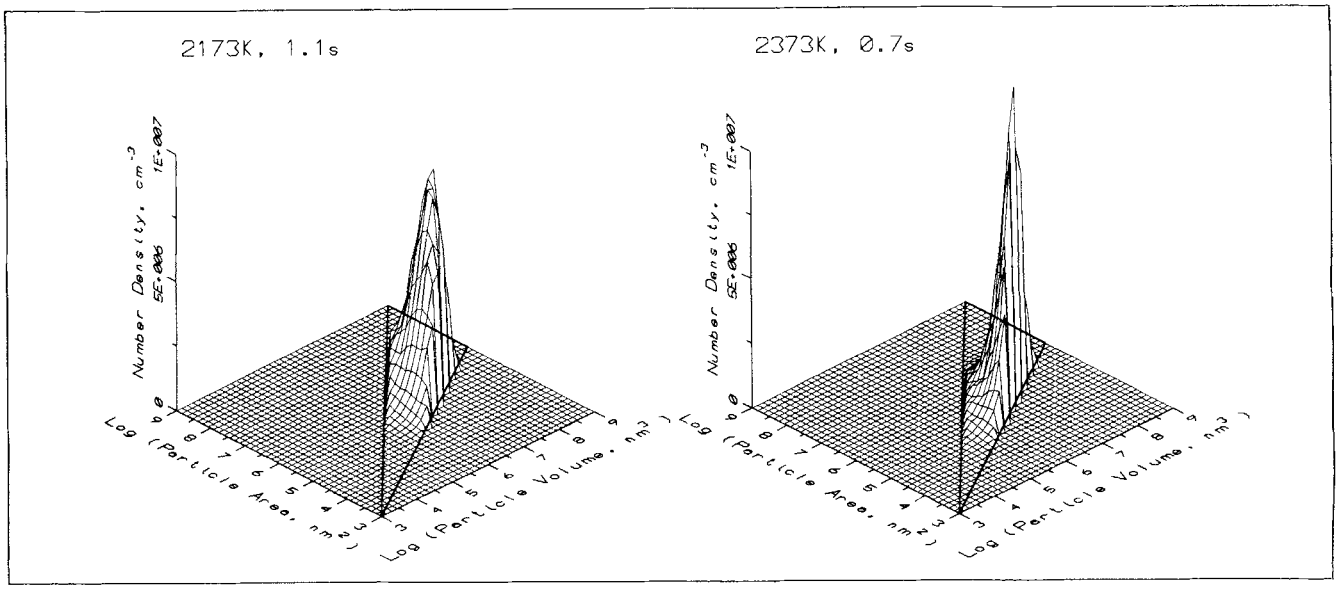

Figure 4. Number density of B_4C agglomerates at 2,173 K and 1.1 s (Run 38-24) and at 2,373 K and 0.7 s (Run 35), respectively, in the two-dimensional space of particle volume and surface area.

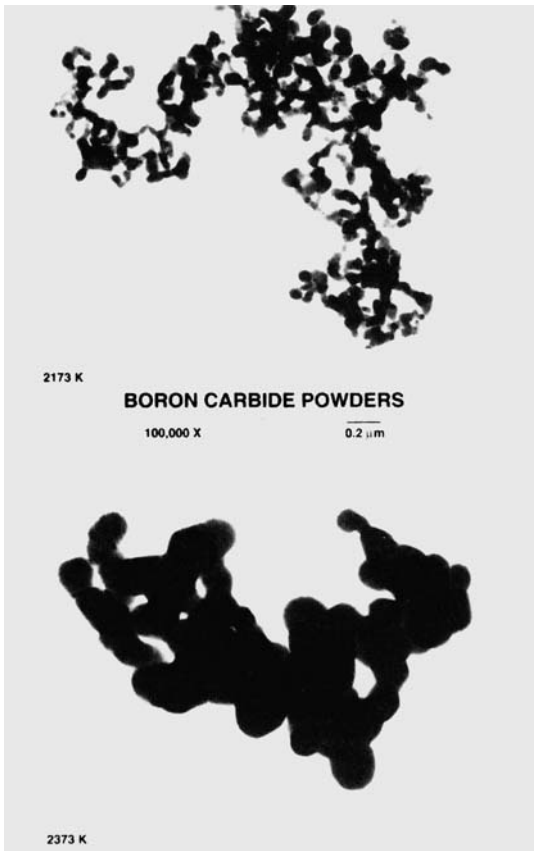

Figure 5. Micrographs of B_4C powders from Run 38-24 (2,173 K) and Run 35 (2,373 K).

corresponds to fully coalesced B_4C particles and is termed the coalescence line. Therefore, the grain size of B_4C agglomerates increases as the initially agglomerated clusters/particles are progressively densified by sintering of the primary particles (grains) in the cluster/particle and the agglomerate particle surface area decreases from the collision to the coalescence line.

Temperature has a much stronger effect on the particle coalescence rate than on the particle collision rate as indicated by the characteristic sintering time of B_4C (Eq. 16). Figure 4 shows two snapshots of the number density of B_4C agglomerates in the two-dimensional space of particle volume and surface area at 2,173 K and 1.1 s (Run 38-24) and at 2,373 K and 0.7 s (Run 35), respectively. The two-dimensional particle size distribution shifts towards the coalescence line as temperature increases indicating more progressed sintering at 2,373 K even though at a shorter residence time. For agglomerates of the same volume, there are relatively more particles having low surface area (large grains, Eq. 18) at high temperatures. If favorable sintering conditions are sustained, the agglomerates eventually approach a spherical geometry and their surface area becomes proportional to $v^{2/3}$ (coalescence line). Indeed, the simulations show that the average B_4C grain size is $d_g = 0.06$ μm at 2,173 K and 1.1 s while at 2,373 K and 0.7 s $d_g = 0.09$ μm. In contrast, the corresponding average equivalent solid sphere diameter of the agglomerate particles is $d_p = 0.44$ μm at 2,173 K and $d_p = 0.37$ μm at 2,373 K at the above residence times. This model prediction is in qualitative agreement with micrographs of B_4C powders made at the above temperatures and shown in Figure 5. There it can be seen that the agglomerate size is roughly the same at both temperatures but the grain sizes are distinctly different.

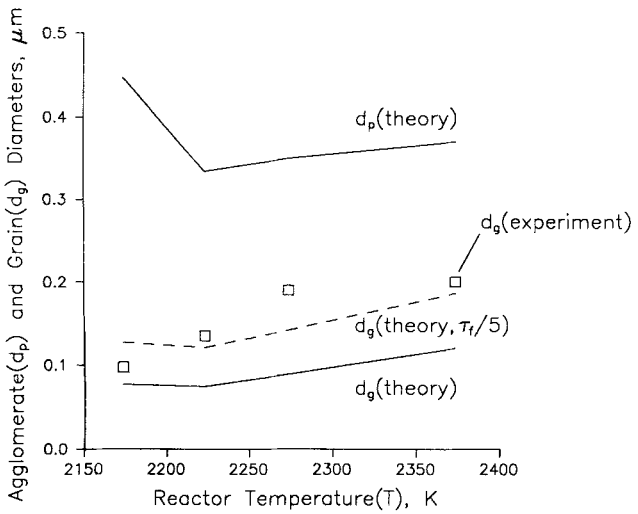

Figure 6. Model predictions of the agglomerate size (d_p) of the B_4C powders as a function of temperature and comparison of the predicted grain size (d_g) with experimental data.

Figure 6 compares theoretical and experimental results for the product B_4C agglomerate (d_p) and grain size (d_g). By simultaneously tracing the change in particle volume and surface area as a result of coagulation and sintering, the present two-dimensional particle size distribution model distinguishes grain size from agglomerate size and predicts the evolution of both d_p and d_g. The top solid line shows model predictions of the equivalent solid sphere diameter of the agglomerate particles (d_p) as a function of temperature at the conditions of the four experimental runs (Table 1). The theoretical agglomerate size at 2,173 K (Run 38-24) is much larger than those at all other temperatures as a result of a lower argon flow rate and hence a longer residence time (Table 1). Figure 6 also compares model predictions of the B_4C average grain diameter (d_g) with experimental data at the 4 runs. Clearly, the equivalent solid sphere diameter of an agglomerate is much larger than the grain size. It is worth noting here that the agglomerate size d_p is relatively insensitive to reactor temperature. In contrast, the temperature has a profound effect on the grain size. Using the characteristic sintering time of Eq. 16 correctly represents the grain growth evolution as a function of temperature (Figure 6, bottom solid line). Quantitative agreement with experimental data (squares) is excellent, in view of the estimated B_4C sintering rate (diffusivity and surface energy) and experimental accuracy of the BET surface area measurement. Increasing the sintering rate (or decreasing the characteristic coalescence time τ_f) by a factor of 5 results in a closer match (dashed line) with the experimental data. Thus, the present two-dimensional particle size distribution model can be used to infer effective sintering rates from experimental measurements. This important implication of the model is particularly valuable for ceramic materials whose sintering rate expressions are often unavailable.

Conclusions

The formation of submicron crystals of boron carbide by coagulation and sintering by the rapid carbothermal reduction of solid precursors in an aerosol flow reactor was modeled. At temperatures above the boiling point of boron oxide (2,133 K) and high heating rates (10^5 K/s), B_4C molecular clusters are formed instantaneously and grow to macroscopic particles by coagulation and coalescence. The process is simulated by a two-dimensional aerosol dynamics model that traces the evolution of both size and shape characteristics of particles through their volume and surface area. Model predictions for the average volume and grain/crystallite size of the product B_4C powders are in agreement with experimental micrographs and specific surface area data. The effect of temperature and residence time on particle size and morphology is also nicely represented by the model. More importantly, the present modeling approach can be used to infer effective sintering rates of aerosol made ceramic powders from specific surface area or micrographic measurements.

Acknowledgment

This research was supported by the National Science Foundation Grant CTS-8957042 and Dow Chemical USA. Computer time and the IMSL software were provided by the Ohio Supercomputer Center.

Notation

a = particle surface area, cm^2
a_{final} = surface area of the final completely fused sphere, cm^2
a_o = primary particle surface area, cm^2
A = specific surface area, cm^2/g
d_a = surface area equivalent sphere diameter of agglomerate particles, cm
d_g = average grain/crystallite size, cm
d_p = equivalent solid sphere diameter of agglomerate particles, cm
D^* = diffusivity, cm^2/s
D_s = surface fractal dimension
F_g = gas feed rate, g/s
F_s = solid feed rate, g/s
i = cluster size (v/v_o)
j = number of surface monomers
k_B = Boltzmann's constant, 1.38×10^{-16} erg/K
$n_f(v, a)$ = two-dimensional particle size distribution function, cm^{-8}
s = surface area accessibility
t = time, s
T = temperature, K
v = particle volume, cm^3
v_o = primary particle volume, cm^3

Greek letters

α = surface area scaling factor
β = collision frequency function, cm^3/s
γ = surface energy, dyne/cm
θ = step function
ρ_p = particle density, g/cm^3
τ_f = characteristic coalescence time, s
Ω = atomic volume of the diffusing species, cm^3

Literature Cited

Cannon, W. R., S. C. Danforth, J. H. Flint, J. S. Haggerty, and R. A. Marra, "Sinterable Ceramic Powders from Laser-Driven Reactions," *J. Am. Ceram. Soc.*, **65**, 324 (1982).

Celik, I., T. J. O'Brien, and D. B. Godbole, "A Numerical Study of Coal Devolatilization in an Entrained-Flow Reactor," *Chem. Eng. Sci.*, **45**(1), 65 (1990).

Dean, J. A., *Lange's Handbook of Chemistry*, 13th ed., McGraw-Hill, New York (1985).

Fuchs, N. A., *The Mechanics of Aerosols*, Pergamon Press, New York (1964).

Gelbard, F., Y. Tambour, and J. H. Seinfeld, "Sectional Representations for Simulating Aerosol Dynamics," *J. Colloid Interf. Sci.*, **76**(2), 541 (1980).
Gray, E. G., "Process for the Production of Boron Carbide," U.S. Pat. 2,834,651 (1958).
Greskovich, C., and J. H. Rosolowski, "Sintering of Covalent Solids," *J. Am. Ceram. Soc.*, **59**(8), 336 (1976).
Hase, T., and H. Suzuki, "Solubility and Diffusion of Si in B_4C," *Commun. Am. Ceram. Soc.*, C58 (1981).
IMSL, *User's Manual*, IMSL Math/Library, Vol. 2, Version 1.1, Houston (1989).
Kingery, W. D., H. K. Bowen, and D. R. Uhlmann, *Introduction to Ceramics*, Wiley, New York (1976).
Koch, W., and S. K. Friedlander, "The Effect of Particle Coalescence on the Surface Area of a Coagulating Aerosol," *J. Colloid Interf. Sci.*, **140**(2), 419 (1990).
Lamoreaux, R. H., D. L. Hildenbrand, and L. Brewer, "High-Temperature Vaporization Behavior of Oxides II. Oxides of Be, Mg, Ca, Sr, Ba, B, Al, Ga, In, Tl, Si, Ge, Sn, Pb, Zn, Cd, and Hg," *J. Phys. Chem. Ref. Data*, **16**(3), 419 (1987).
Lange, F. F., and T. K. Gupta, "Sintering of SiC with Boron Compounds," *J. Am. Ceram. Soc.*, **59**(11), 537 (1976).
Lipp, A., "Boron Carbide: Production, Properties, Applications," *Tech. Rundschau*, **28**(14), 33 (1965).
Livey, D. T., and P. Murray, "Surface Energies of Solid Oxides and Carbides," *J. Am. Ceram. Soc.*, **39**(11), 363 (1956).
Mackinnon, I. M., and B. G. Reuben, "The Synthesis of Boron Carbide in an RF Plasma," *J. Electrochem. Soc.*, **122**(6), 806 (1975).
Mandelbrot, B. B., *The Fractal Geometry of Nature*, W. H. Freeman and Company, New York (1983).
Meakin, P., and T. A. Witten, Jr., "Growing Interface in Diffusion-Limited Aggregation," *Phys. Rev. A.*, **28**, 2985 (1983).
Meakin, P., "Effects of Cluster Trajectories on Cluster-Cluster Aggregation: A Comparison of Linear and Brownian Trajectories in Two- and Three-Dimensional Simulations," *Phys. Rev. A*, **29**(2), 997 (1984).
Osipov, D., "Effect of Porosity and Grain Size on the Mechanical Properties of Hot-Pressed Boron Carbide," *Sov. Powder Metall. Met. Ceram.* (Engl. trans.), **21**(1), 55 (1982).
Reid, R. C., J. M. Prausnitz, and B. E. Poling, *The Properties of Gases & Liquids*, 4th ed., McGraw-Hill, New York (1987).
Schaefer, D. W., and A. J. Hurd, "Growth and Structure of Combustion Aerosols: Fumed Silica," *Aerosol Sci. Technol.*, **12**, 876 (1990).
Schmidt-Ott, A., "New Approaches to *In Situ* Characterization of Ultrafine Agglomerates," *J. Aerosol Sci.*, **19**(5), 553 (1988).
Seinfeld, J. H., *Atmospheric Chemistry and Physics of Air Pollution*, Wiley, New York (1986).
Thevenot, F., "Sintering of Boron Carbide and Boron Carbide-Silicon Carbide Two-Phase Materials and Their Properties," *J. Nucl. Mat.*, **152**, 154 (1988).
van Rijswijk, W., and D. J. Shanefield, "Effects of Carbon as a Sintering Aid in Silicon Carbide," *J. Am. Ceram. Soc.*, **73**(1), 148 (1990).
Weast, R. C., M. J. Astle, and W. H. Beyer, *CRC Handbook of Chemistry and Physics*, 6th ed., CRC Press, Florida (1986).
Weimer, A. W., W. G. Moore, R. P. Roach, C. N. Haney, and W. Rafaniello, "Rapid Carbothermal Reduction of Boron Oxide in a Graphite Transport Reactor," *AIChE J.*, **37**, 759 (1991).
Weimer, A. W., W. G. Moore, R. P. Roach, J. E. Hitt, R. S. Dixit, and S. E. Pratsinis, "Kinetics of Carbothermal Reduction Synthesis of Boron Carbide," *J. Amer. Ceram. Soc.*, **75**(9), 2509 (1992).
Xiong, Y., and S. E. Pratsinis, "Gas Phase Production of Particles in Reactive Turbulent Flows," *J. Aerosol Sci.*, **22**(5), 637 (1991a).
Xiong, Y., and S. E. Pratsinis, "Formation of Irregular Particles by Coagulation and Sintering: A Two-Dimensional Solution of the Population Balance Equation," Proceedings of the 1991 European Aerosol Conference, *J. Aerosol Sci.*, **22** (Suppl. 1), s199 (1991b).
Xiong, Y., *Dynamics of Particle Formation and Growth in Gas Phase Processes*, PhD Thesis, University of Cincinnati (1992).
Xiong, Y., and S. E. Pratsinis, "Particle Formation by Coagulation and Sintering. Part I: A Two-Dimensional Solution of the Population Balance Equation," *J. of Aerosol Sci.*, in press (1993).
Xiong, Y., M. K. Akhtar, and S. E. Pratsinis, "Particle Formation by Coagulation and Sintering. Part II: The Evolution of the Morphology of Aerosol Made Titania, Silica and Silica-Doped Titania Powders," *J. of Aerosol Sci.*, in press (1993).

Manuscript received March 10, 1992, and revision received June 15, 1992.